

Demographic noise as a triggering mechanism for algal blooms

Piero Olla

ISAC-CNR and INFN, Sez. Cagliari, I-09042 Monserrato, Italy.

(Dated: February 25, 2019)

Population models, such as those for plankton dynamics, are often based on a mean-field approximation of individual behaviors. A weakly stable mean-field configuration, however, can be destabilized by demographic noise. In certain cases, such destabilization persists even in the thermodynamic limit. The possible relevance of such an effect to the onset of algal blooms is discussed.

PACS numbers: 87.23.Cc, 87.10.Mn, 02.50.Ey, 05.40.-a

I. INTRODUCTION

Phytoplankton provide the basis of the food chain in the ocean. They are constituted for the large part by microscopic algae and their abundance is such that they are responsible for roughly one half of the total photosynthesis going on in the planet [1].

Although phytoplankton are present in virtually all of the world hydrosphere (more precisely, the top 100 m layer of the water column, called the euphotic layer, where there is enough light for photosynthesis), their distribution in space and time is far from uniform [2]. Space patchiness is observed at scales that go from that of the individual to several hundreds kilometers [3, 4]. The spatial patterns, revealed e.g. by remote sensing, include filaments, fronts and more irregular shapes, suggesting that turbulent transport by sea currents may play an important role [5–9].

Variability in time, on the other hand, is characterized by sporadic bloom events in which the plankton density in extended regions can grow by up to three orders of magnitude in few days [10]. These are seasonal events that may or may not recur annually, and are superimposed to the weaker day-night and seasonal cycles. Their importance is utmost for several reasons. Depending on the species (e.g. diatoms), due to their abundance, bloom events can have consequences even at the level of the global biogeochemical cycle [11]. Bloom events involving other species (e.g. dinoflagellates) can have harmful effects on water quality and fishery [12, 13]. Being able to predict the onset of algal blooms is clearly an issue of great practical importance.

Several mechanisms of both biological and physical nature contribute to blooms, not all of them probably known yet. From the point of view of biology, the dominant controlling factor for phytoplankton growth is usually considered to be grazing by zooplankton [14] (though nutrient transport, light, and the presence of a thermocline surely play an important role [15]). This is the so called mismatch issue [16]: since the life cycle of phytoplankton is typically one order of magnitude shorter than that of zooplankton, a positive fluctuation in phytoplankton productivity is not compensated by a simultaneous increase in the zooplankton population. This produces the bloom event: the phytoplankton population escapes

zooplankton control and grows to the carrying capacity of the medium, before also the zooplankton population grows appreciably, and is able to bring that of the phytoplankton back to its pre-bloom level.

At a sufficiently coarse grained scale, the system dynamics can be described by phytoplankton and zooplankton concentration fields $\bar{P}(\mathbf{x}, t)$ and $\bar{Z}(\mathbf{x}, t)$ [17, 18]. This constitutes a mean field approximation for the stochastic individual dynamics; at different levels of complexity, such a description may include the nutrient and even the detritus concentration fields $\bar{N}(\mathbf{x}, t)$ and $\bar{D}(\mathbf{x}, t)$ (NPZ [19, 20] and NPZD [21] models). The tininess of both phyto- and zooplankton individuals, as well as the size of typical areas of interest for the study of the concentration dynamics (at least several meters), suggests that a mean field description is indeed the most appropriate. The fact that bloom events may be triggered by fluctuations in the system, however, should suggest caution.

The point that we want to examine in the present paper is precisely whether microscopic fluctuations, disregarded in a mean field approach, can resurface at macroscopic scale and contribute to trigger bloom events. This is an example of demographic fluctuation induced breakdown of mean field descriptions of reaction-diffusion systems, a type of phenomenon that have received a great deal of attention in recent years [22–26]

In the present paper we shall consider a simple PZ model due to Truscott and Brindley (TB model), which has the nice characteristics that the plankton behaves like an excitable medium [18]. The original model is zero-dimensional, but can be easily generalized to include spatial effects such as advection and diffusion [27]. In the present analysis a spatially homogeneous domain will be considered with no advection, but with diffusive terms accounting for small scale motions in the water column. The game to play will be to determine the demographic fluctuations implicitly neglected in the TB model, and see if they can destabilize the system even at the level of spatial averages.

This paper is organized as follows. In Sec. II, the main properties of the TB model are reviewed. In Sec. III, the expression for the stochastic contribution to demography are derived. In Sections IV and V, the effect of demographic noise on the dynamics of the TB model, without and with seasonal forcing, is analyzed. Section VI is devoted to the conclusions. Some technical details

on the master equation treatment of demographic fluctuations, in spatially extended domains, are provided in the Appendix for reference.

II. THE TRUSCOTT-BRINDLEY MODEL

We review here the main properties of the TB model. For the moment we disregard the spatial structure of the fields and focus on the original zero-dimensional version of the model, which is described by the equations:

$$\begin{aligned}\dot{\bar{P}} &= r_0\bar{P}\left(1 - \frac{\bar{P}}{K}\right) - R_m\frac{\bar{P}^2\bar{Z}}{\bar{P}^2 + \alpha^2}, \\ \dot{\bar{Z}} &= -\mu\bar{Z} + \gamma R_m\frac{\bar{P}^2\bar{Z}}{\bar{P}^2 + \alpha^2}.\end{aligned}\quad (1)$$

The main characteristics of the dynamics are the following:

- Logistic reproductive behavior of the phytoplankton, with the carrying capacity K determining the maximum concentration that the medium can support at steady state.
- Grazing by zooplankton characterized by a so called Holling-III kind of behavior [28]. Zooplankton are able to graze on phytoplankton with optimal rate $R_m\bar{Z}$, only if the concentration of the second is above the level fixed by the half-saturation concentration α . Below this threshold, the grazing rate is quadratic in \bar{P} : $R_m(\bar{P}/\alpha)^2\bar{Z}$, reflecting both a reduced grazing ability of the zooplankton in a dilute environment, and the actual reduced amount of food available.
- A carrying capacity of the medium supposed much larger than the half saturation concentration, $K \gg \alpha$, meaning that at high values of \bar{P} , the ability of zooplankton to control phytoplankton growth is limited.
- A zooplankton reproductive dynamics supposed slower than that of the phytoplankton: $\mu/R_m \ll 1$, while $r_0/R_m \sim 1$. A conversion efficiency γ assumed consistently small.

The default values of the constants that are utilized in the zero-dimensional case are [18]:

$$\begin{aligned}r_0 &= 0.3/\text{day}, & R_m &= 0.7/\text{day}, & \mu &= 0.012/\text{day}, \\ K &= 108\text{mg C}/\text{m}^3, & \alpha &= 5.7\text{mg C}/\text{m}^3, \\ \gamma &= 0.05,\end{aligned}\quad (2)$$

where the units “mg C” stand for carbon milligrams in dry weight. From here we can extract three independent dimensionless groups

$$\begin{aligned}\hat{r}_0 &= \frac{r_0}{R_m} \simeq 0.43, & q &= \frac{\mu}{\gamma R_m} \simeq 0.34, \\ \epsilon &= \frac{\alpha}{K} \simeq 0.053.\end{aligned}\quad (3)$$

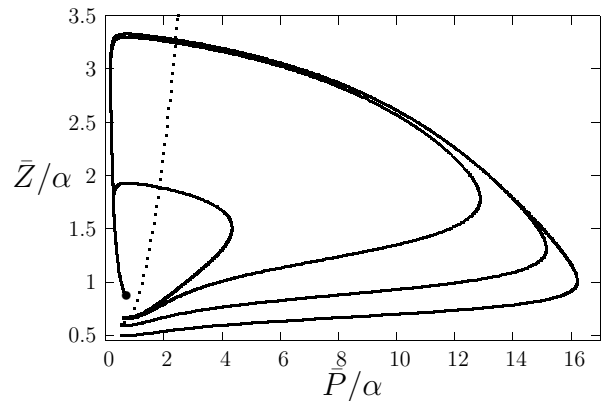


FIG. 1: Trajectories approaching the fixed point (P_f, Z_f) (fat dot to lower left corner of picture) starting from different initial conditions; going from outer to inner trajectory: $(\bar{P}, \bar{Z}) = (0.5, 0.5)$; $(0.5, 0.6)$; $(0.6, 0.66)$; $(0.6, 0.68)$. The parameters are those of Eq. (2). The dotted line indicate change of signature of the Jacobian matrix for Eq. (1), and could roughly be identified as the point where the bloom begins.

We see that the dynamics is characterized by two independent small parameters: γ and ϵ . The dynamics described by Eq. (1) has a fixed point at the scale of the half-saturation constant α :

$$\begin{aligned}P_f &= \alpha\sqrt{\frac{q}{1-q}}, \\ Z_f &= \frac{\hat{r}_0}{P_f}\left(1 - \frac{P_f}{K}\right)(\alpha^2 + P_f^2) \simeq \frac{\alpha\hat{r}_0}{\sqrt{q(1-q)}}.\end{aligned}\quad (4)$$

For small $\gamma, \epsilon \ll 1$ and $q < 1/2$, this fixed point is globally attracting (a Holling-III functional form for grazing appears to be crucial for stability). However, if the initial zooplankton concentration is too low, before reaching the fixed point, the system will make an excursion to the high $\bar{P} \sim K$ range, which could be interpreted as a bloom event. The situation is illustrated in Fig. 1. As shown in figure, the onset of bloom could roughly be identified in the $\bar{P}\bar{Z}$ plane by the line where the largest eigenvalue of the Jacobian of Eq. (1) crosses to positive, and phase points start to separate exponentially.

The above picture of bloom triggering by zooplankton depletion can be improved including the effect of seasonal forcing. Model equations (1) can accommodate this effect by letting the phytoplankton productivity r become dependent on the temperature, as suggested in [29]. The parameterization that we adopt is the same as in [29]: a Van't Hoff kind of dependence for r [30]:

$$r_0 \rightarrow r(T) = r_0 2^{v(T-T_0)} \quad (5)$$

and a sinusoidal dependence on time of the temperature:

$$T(t) = T_0 + \Delta T \sin(\Omega t + \phi). \quad (6)$$

with $\Omega = 2\pi/(365 \text{ days})$ to allow for an annual cycle, and $\phi/(2\pi) = 0.59$, to have that setting $t = 0$ on January

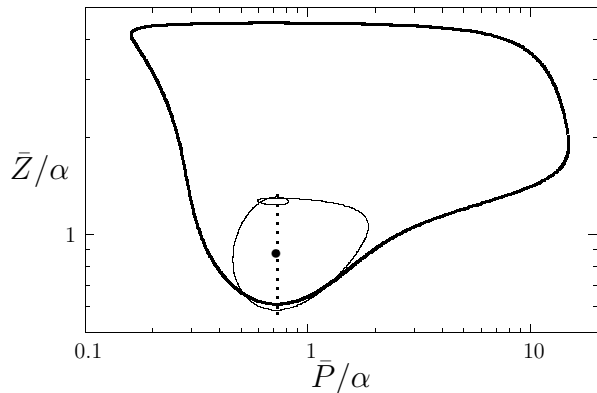


FIG. 2: Bloom and no-bloom cycles (heavy and thin lines respectively) in the seasonally forced TB model. The phase points circle counterclockwise along the cycle. Notice that the intersections of the two cycles corresponds to these points that in the two cycles are associated to different (although close) instants of time. The dotted vertical line gives the position of the fixed points that would correspond to the different values taken by \hat{r} during the year. The fat dot still identifies the fixed point corresponding to $\hat{r} = \hat{r}_0$. The parameters in the graph are those in Eqs. (5-6).

1st, causes the first temperature minimum to occur on March 1st and the first maximum on August 29th. For the sake of definiteness, as in ..., we set $\Delta T = 6^\circ\text{C}$ and $\nu = 0.1^\circ\text{C}^{-1}$.

Adding a seasonal forcing, turns out to modify the dynamics in important way, with the single fixed point in the autonomous case leaving way to two stable limit cycles [29]. The situation is illustrated in Fig. 2: a small amplitude no-bloom cycle coexists with a large amplitude bloom cycle, each one characterized by a well defined (time-dependent) basin of attraction. As illustrated in Fig. 3, the small cycle will remain stable only if the seasonal temperature excursion ΔT is below a critical threshold $\Delta T_{crit}(\hat{r}_0, q, \epsilon, \gamma)$, that, for the values of the parameters quoted in Eqs. (2) is $\Delta T_{crit} \simeq 6.1^\circ\text{C}$. Similarly, it can be shown that, if ΔT is too small, only the no-bloom cycle will survive. The no-bloom destabilization threshold is very close to the value of the forcing $\Delta T = 6^\circ\text{C}$ considered in [29]. The analysis in that paper showed in fact that addition of a fluctuating component to the forcing, lead to random switch from year to year between the two regimes. As it is clear from Fig. 2, the destabilization is likely to take place near the intersection between the bloom and no-bloom trajectories, where the separation between the phase points of the two cycles (at equal times) is smaller.

III. DEMOGRAPHIC FLUCTUATIONS

We consider a situation in which the typical size of a zooplankton individual is much larger than that of a typ-

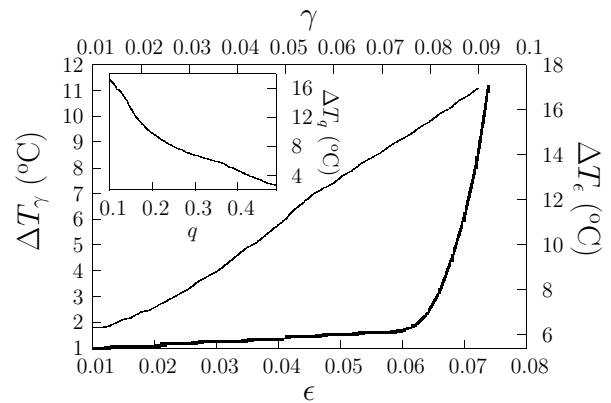


FIG. 3: Dependence on the critical forcing amplitude ΔT_{crit} on the parameters γ (thin line), ϵ (heavy line) and q (insert). In the three cases $\Delta T_{\gamma, \epsilon, q}$ indicate the value of ΔT_{crit} obtained varying γ, ϵ, q respectively and keeping the remaining parameters fixed to the values in Eq. (3).

ical phytoplankter. A reasonable estimate (with large variations) for the mass of a copepod could be, for instance:

$$m_Z \sim 20 \mu\text{g C}, \quad (7)$$

corresponding to a typical individual size in the millimeter range [6, 31]. In a no-bloom regime $\bar{P}, \bar{Z} \sim \alpha$ with α given as in Eq. (2), Eq. (7) would lead to a numerical density of the order of one zooplankton individual per liter. Given the much smaller size of microscopic algae, phytoplankton could in turn be treated as a continuum at those scales. We thus expect that the demographic fluctuations in the system be driven by the zooplankton.

Locally, demographic fluctuations will be the result of a competition between stochasticity at the individual level of the birth-death process, and mixing by spatial transport. We shall consider a two-dimensional situation, in which the vertical structure of the water column is not resolved, and parameterize horizontal mixing through a diffusivity κ , supposed equal for both phyto- and zooplankton. This is probably the only viable strategy to describe a very complex situation, in which microscopic swimming, stirring by larger organisms, turbulence generated by perturbations at the water surface, all play an important role [32]. Likewise, we shall neglect all effects of large scale advection, including the forcing induced by the formation of fronts, where the two plankton populations may get out of balance [5].

Including the possibility of a 2D spatial structure, the original model equations (1) can be written in the form

$$\begin{aligned} \dot{\bar{P}} &= B_P(\bar{P}, \bar{Z}) - D_P(\bar{P}, \bar{Z}) + \kappa \nabla^2 \bar{P}, \\ \dot{\bar{Z}} &= B_Z(\bar{P}, \bar{Z}) - D_Z(\bar{P}, \bar{Z}) + \kappa \nabla^2 \bar{Z}, \end{aligned} \quad (8)$$

where B_{PZ} and D_{PZ} give the local birth and death rates in the population, and $\bar{P} = \bar{P}(\mathbf{x}, t)$ and $\bar{Z} = \bar{Z}(\mathbf{x}, t)$ give

the plankton concentration averaged over the height of the water column. Expressing time in units R_m^{-1} and concentrations in units α (and lengths in terms of some reference scale), the parameters entering Eq. (8) can be written in the form

$$\begin{aligned} B_P &= \hat{r}\bar{P}; & D_P &= \epsilon\hat{r}\bar{P}^2 + \bar{P}^2\bar{Z}/(1 + \bar{P}^2); \\ B_Z &= \gamma\bar{P}^2\bar{Z}/(1 + \bar{P}^2); & D_Z &= \gamma q\bar{Z}. \end{aligned} \quad (9)$$

From now on, unless otherwise stated, all relations will be expressed in dimensionless form.

Rather than working in a field theoretical setting [33], we prefer to apply the standard system size expansion approach of van Kampen directly to the master equation for the system [34]. Let us therefore partition the domain in volumes of horizontal size Δx , each one containing instantaneously N_P, N_Z individuals of the P and Z groups. We can introduce instantaneous concentrations $P, Z = \Omega_{P,Z}^{-1} N_{P,Z}$, coarse grained at horizontal scale Δx , with

$$\Omega_{P,Z} = h(\Delta x)^2 / m_{P,Z} \quad (10)$$

parameterizing the size of the population in the volumes, and h indicating the height of the water column. Indicate with $\tilde{P} = P - \bar{P}$ and $\tilde{Z} = Z - \bar{Z}$ the fluctuating part of the coarse-grained field; in the present situation of fluctuations driven by zooplankton discreteness, we expect $\tilde{P}/\bar{P}, \tilde{Z}/\bar{Z} = O(N_Z^{-1/2})$. Let us define normalized fluctuation fields ϕ, ζ with this scaling contribution factored out:

$$\begin{aligned} N_P &= \Omega_P P := \Omega_P (\bar{P} + \Omega_Z^{-1/2} \phi), \\ N_Z &= \Omega_Z Z := \Omega_Z (\bar{Z} + \Omega_Z^{-1/2} \zeta). \end{aligned}$$

The standard approach is to hypothesize that the birth and death rates $B_{P,Z}$ and $D_{P,Z}$ at the population scale, reflect birth and death rates at the individual level, conditioned to the instantaneous values of the concentration fields $P(\mathbf{x}, t)$ and $Z(\mathbf{x}, t)$. At the population level, the transition probabilities $d\mathcal{P}$ in an interval dt will be:

$$\begin{aligned} N_P \rightarrow N_P + 1 : & d\mathcal{P} = \Omega_P B_P(P, Z) dt, \\ N_P \rightarrow N_P - 1 : & d\mathcal{P} = \Omega_P D_P(P, Z) dt, \\ N_Z \rightarrow N_Z + 1 : & d\mathcal{P} = \Omega_Z B_Z(P, Z) dt, \\ N_Z \rightarrow N_Z - 1 : & d\mathcal{P} = \Omega_Z D_Z(P, Z) dt. \end{aligned} \quad (11)$$

A standard procedure [34] leads then, from Eq. (11), to the master equation for the probability density function (PDF) $\rho(\{\phi_i, \zeta_i\}, t)$ (the index i labels the volumes in the

domain):

$$\begin{aligned} \frac{\partial \rho}{\partial t} &= \sum_i \left\{ \Pi_i \rho + \Omega_Z^{1/2} \left[\dot{\tilde{P}}_i \frac{\partial \rho}{\partial \phi_i} + \dot{\tilde{Z}}_i \frac{\partial \rho}{\partial \zeta_i} \right] \right. \\ &+ \Omega_P \left\{ \left[\exp \left(-\Omega_C^{-1/2} \frac{\partial}{\partial \phi_i} \right) - 1 \right] B_{P,i} \right. \\ &+ \left. \left[\exp \left(\Omega_C^{-1/2} \frac{\partial}{\partial \phi_i} \right) - 1 \right] D_{P,i} \right\} \rho \\ &+ \Omega_Z \left\{ \left[\exp \left(-\Omega_Z^{-1/2} \frac{\partial}{\partial \zeta_i} \right) - 1 \right] B_{Z,i} \right. \\ &+ \left. \left[\exp \left(\Omega_Z^{-1/2} \frac{\partial}{\partial \zeta_i} \right) - 1 \right] D_{Z,i} \right\} \rho \left. \right\}, \end{aligned} \quad (12)$$

where $\Omega_C^{1/2} = \Omega_Z^{-1/2} \Omega_P$, and the additional term $\Pi_i \rho$ accounts for the exchange of plankton between adjacent volumes produced by diffusion (see Appendix). Expanding to lowest order in $\Omega_{P,Z}^{-1}$, both the exponentials and the reaction rates in Eq. (12) [recall that $B_P = B_P(\bar{P} + \Omega_Z^{-1/2} \phi, \bar{Z} + \Omega_Z^{-1/2} \zeta), \dots$], we obtain the Fokker-Planck equation:

$$\begin{aligned} \frac{\partial \rho}{\partial t} &+ \sum_i \left\{ \frac{\partial}{\partial \phi_i} (a_{PP,i} \phi_i + a_{PZ,i} \zeta_i) \rho \right. \\ &+ \left. \frac{\partial}{\partial \zeta_i} (a_{ZP,i} \phi_i + a_{ZZ,i} \zeta_i) \rho \right\} \\ &= \sum_i \Pi_i \rho + \frac{1}{2} \sum_{ij} \frac{\partial}{\partial \zeta_i} \frac{\partial}{\partial \zeta_j} \Xi_{ij} \rho, \end{aligned} \quad (13)$$

where $\Xi_{ij} = [B_Z(\bar{P}_i, \bar{Z}_i) + D_Z(\bar{P}_i, \bar{Z}_i)] \delta_{ij}$, and the a_{PP}, \dots give the entries of the Jacobian matrix for Eq. (1) ($a_{PP} \equiv \partial \dot{\tilde{P}} / \partial \bar{P}, \dots$). Notice that the only noise correlator present in the equation, Ξ_{ij} , is the one associated with the variable ζ , i.e. with the zooplankton fluctuations.

Going back to the original variables \tilde{P}, \tilde{Z} , and taking the continuous limit, we see that the Fokker-Planck equation (13) is equivalent to the system of Langevin equations

$$\begin{aligned} \frac{\partial \tilde{P}}{\partial t} + a_{PP} \tilde{P} + a_{PZ} \tilde{Z} &= \kappa \nabla^2 \tilde{P} \\ \frac{\partial \tilde{Z}}{\partial t} + a_{ZP} \tilde{P} + a_{ZZ} \tilde{Z} &= \kappa \nabla^2 \tilde{Z} + \xi, \end{aligned} \quad (14)$$

where

$$\begin{aligned} \langle \xi(\mathbf{x}, t) \xi(0, 0) \rangle &= \Xi(\mathbf{x}, t) \delta(\mathbf{x}) \delta(t), \\ \Xi(\mathbf{x}, t) &= \hat{m}_Z [B_Z(\bar{P}, \bar{Z}) + D_Z(\bar{P}, \bar{Z})], \end{aligned} \quad (15)$$

and we have put $\hat{m}_Z = m_Z/h$, $\bar{P} \equiv \bar{P}(\mathbf{x}, t)$ and $\bar{Z} \equiv \bar{Z}(\mathbf{x}, t)$ (more details in the Appendix).

Equations (13-15) provide a mesoscopic description for the system dynamics that is valid as long as the fluctuations at scale Δx can be considered small. It is immediately clear that this condition cannot be satisfied in a

bloom regime. In fact, as illustrated in Fig. 1, bloom is associated with change of signature in the Jacobian matrix of Eq. (1) and with exponential growth of fluctuations in Eq. (14). We shall deal with this regime in Sec. V; let us concentrate for the moment the case of small fluctuations.

IV. DYNAMICS NEAR THE FIXED POINT

Let us consider first the case of a TB model without seasonal forcing, and study the fluctuations around the fixed point given by Eq. (4). The analysis is similar to the one carried on in [26] on another PZ model (the Levin-Segel model [35]), which focused on the destabilization of Turing patterns. The evolution equations for the correlation functions $C_{PP}(\mathbf{x}, t) = \langle \tilde{P}(\mathbf{x}, t) \tilde{P}(0, t) \rangle, \dots$ can be obtained from Eqs. (14-15), and take the form in Fourier space:

$$\begin{aligned} \frac{1}{2} \dot{C}_{PP\mathbf{k}} + (a_{PP} + \kappa k^2) C_{PP\mathbf{k}} + a_{PZ} C_{PZ\mathbf{k}} &= 0 \\ \dot{C}_{PZ\mathbf{k}} + a_{ZP} C_{PP\mathbf{k}} + (a_{PP} + a_{ZZ} + 2\kappa k^2) C_{PZ\mathbf{k}} \\ + a_{PZ} C_{ZZ\mathbf{k}} &= 0 \\ \frac{1}{2} \dot{C}_{ZZ\mathbf{k}} + a_{ZP} C_{PZ\mathbf{k}} + (a_{ZZ} + \kappa k^2) C_{ZZ\mathbf{k}} &= \Xi. \end{aligned} \quad (16)$$

At the fixed point we find immediately, using Eq. (9) and working to lowest order in ϵ and γ :

$$\begin{aligned} a_{PP} &\simeq -\hat{r}(1-2q), & a_{PZ} &= -q, \\ a_{ZP} &\simeq 2\gamma\hat{r}(1-q), & a_{ZZ} &= 0, \\ \Xi &\simeq 2\gamma\hat{m}_Z \sqrt{q/(1-q)}. \end{aligned} \quad (17)$$

Equation (16) becomes at steady state:

$$\begin{aligned} (a_{PP} + \kappa k^2) C_{PP\mathbf{k}} + a_{PZ} C_{PZ\mathbf{k}} &= 0, \\ a_{ZP} C_{PP\mathbf{k}} + (a_{PP} + 2\kappa k^2) C_{PZ\mathbf{k}} + a_{PZ} C_{ZZ\mathbf{k}} &= 0, \\ a_{ZP} C_{PZ\mathbf{k}} + \kappa k^2 C_{ZZ\mathbf{k}} &= \Xi, \end{aligned}$$

that has solution

$$\begin{aligned} C_{PP\mathbf{k}} &\simeq \Delta^{-1} a_{PZ}^2 \Xi, \\ C_{PZ\mathbf{k}} &\simeq \Delta^{-1} a_{PZ} (-a_{PP} + \kappa k^2) \Xi, \\ C_{ZZ\mathbf{k}} &\simeq \Delta^{-1} (-a_{PP} + \kappa k^2)^2 \Xi, \end{aligned} \quad (18)$$

with

$$\Delta = a_{PP} a_{PZ} a_{ZP} + a_{PP}^2 \kappa k^2 - 2a_{PP} \kappa^2 k^4 + \kappa^3 k^6. \quad (19)$$

From Eqs. (18-19), we see that there is a long wavelength range, dominated by demography; using Eq. (17):

$$\begin{aligned} C_{PP\mathbf{k}} &\simeq \frac{q\hat{m}_Z}{\hat{r}_0^2(1-q)(1-2q)} \sqrt{\frac{q}{1-q}}, \\ C_{PZ\mathbf{k}} &\simeq \frac{\hat{m}_Z}{\hat{r}_0(1-q)} \sqrt{\frac{q}{1-q}}, \\ C_{ZZ\mathbf{k}} &\simeq \frac{\hat{m}_Z(1-2q)}{q(1-q)} \sqrt{\frac{q}{1-q}}. \end{aligned} \quad (20)$$

At small scales, the fluctuations are smeared out by diffusion, with the asymptotic law $C_{PP\mathbf{k}} \simeq a_{PP}^2 \Xi / (\kappa k^2)^3$, $C_{PZ\mathbf{k}} \simeq a_{PZ} \Xi / (\kappa k^2)^2$, $C_{ZZ\mathbf{k}} \simeq \Xi / (\kappa k^2)$. The transition occurs at $\kappa k^2 \sim a_{ZP} a_{PZ} / a_{PP}$, which sets the crossover length, from Eqs. (3) and (17), back to dimensional units:

$$\lambda_c = \sqrt{\kappa/\mu}. \quad (21)$$

This is the typical distance travelled by a zooplankter in a lifetime and corresponds to the characteristic wavelength of the chemical waves supported by the system in the mean field. Notice that, contrary to the case considered in [27], for the choice of parameters utilized, no Turing instability is present.

The correlation spectrum that has been obtained, characterized by a plateau at $k\lambda_c < 1$, and a decay at $k\lambda_c > 1$, corresponds to fluctuations with a correlation scale λ_c . The fluctuation amplitude can be estimated approximating the decay at $k\lambda_c > 1$ with a step function and approximating the solution for $k\lambda_c < 1$ with Eq. (20). This gives for the fluctuation amplitude

$$C_{PP}(0) = \mathcal{F}_{\mathbf{x}=0}^{-1}[C_{PP\mathbf{k}}] \sim \lambda_c^{-2} C_{PP0},$$

with C_{PP0} as given in Eq. (20), and similar expressions for $C_{PZ}(0)$ and $C_{ZZ}(0)$. From Eqs. (20) we get for the ratio of the fluctuation amplitude to the mean (back to dimensional units):

$$\frac{C_{PP}(0)}{\bar{P}^2} \sim \frac{C_{PZ}(0)}{\bar{P}\bar{Z}} \sim \frac{C_{ZZ}(0)}{\bar{Z}^2} \sim \frac{m_Z}{\alpha h \lambda_c^2}, \quad (22)$$

that is the ratio of the zooplankter mass and the typical total plankton mass in a water column of height h and horizontal extension λ_c .

V. DESTABILIZATION OF THE NO-BLOOM REGIME

Let us pass to consider a seasonally forced situation and ask whether demographic noise is able to destabilize the global bloom and no-bloom cycles.

As already discussed, the linearized theory of Sec. IV cannot be utilized in the present case, as the trajectories evolve for most of their time in an unstable region. Thus, numerical solution of the master equation (12) becomes necessary, either by direct means, or by Monte-carlo techniques. In alternative, one may try to extend the Langevin equation (14) beyond the linear regime by replacing the Jacobian matrix a_{ij} with the full RHS (right hand side) of the mean field TB model (8). It is convenient to express lengths in units λ_c , so that the forced equation can be written in the form

$$\begin{aligned} \dot{P} &= B_P(P, Z) - D_P(P, Z) + \lambda q \nabla^2 P, \\ \dot{Z} &= B_Z(P, Z) - D_Z(P, Z) + \lambda q \nabla^2 Z + \xi. \end{aligned} \quad (23)$$

[Notice the dependence of the terms on RHS of Eq. (23) on the fluctuating fields P and Z ; similarly, the dependence on \bar{P} and \bar{Z} in Eq. (15) is replaced by one on P and Z].

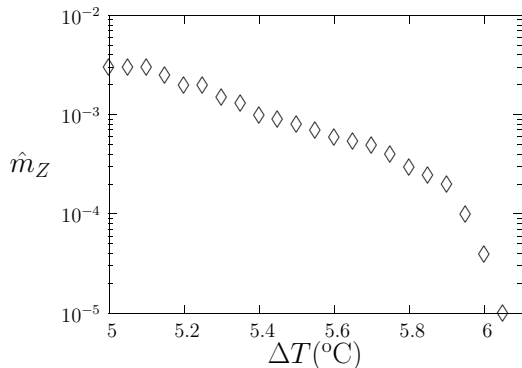


FIG. 4: No-bloom cycle destabilization threshold in function of ΔT , from numerical simulation in a periodic domain $200\Delta X \times 200\Delta X$ with $\Delta X = \lambda_c/10$. The no-bloom cycle is considered destabilized if the system crosses the threshold $\bar{P} = 10$ before $t = 10$ years. All parameters except ΔT and \hat{m}_Z set to the values in Eqs. (2) and (7). Initial conditions set equal to (P_f, Z_f) uniformly in the domain.

In this way, the role of effective diffusivity is played by the product λq , while the parameter \hat{m}_Z , which, through Eq. (15), determines the amplitude of the noise ξ , takes the form, in terms of dimensional parameters:

$$\hat{m}_Z = \frac{m_Z \mu}{\alpha h \kappa}. \quad (24)$$

This quantity will play the role of a control parameter for the theory. [We notice by the way that \hat{m}_Z coincides with the amplitude ratio in Eq. (22)].

The approximation leading to Eq. (23) is clearly uncontrolled, as no account is taken of the modifications produced in the noise term. Nevertheless, except for very large values of \hat{m}_Z , Montecarlo simulation with Eq. (11), and direct solution of Eq. (23), have given very close results. This appears to be due the fact that the noise plays a crucial role in destabilizing the cycles, only in the narrow regions around the “intersections” (see Fig. 2). In the unstable regions, the dynamics is dominated by amplification of the separation between phase points produced by the deterministic part of the equation; the noise plays in the unstable regions a minor role. Thus, the fact that in these regions the noise in Eq. (23) is not well approximated, does not produce dangerous effects.

As expected, a sufficiently high level of noise destabilizes the small cycle and leads to locking the system in the large bloom cycle. As illustrated in Fig. 4, the threshold in \hat{m}_Z becomes lower as the critical forcing ΔT_{crit} is approached.

For default values of the parameters, such as those in Eqs. (2) and (7), with $\Delta T = 6^\circ\text{C}$, the threshold would be at $\hat{m}_Z \simeq 4 \cdot 10^{-5}$, which, for a depth $h \simeq 5$ m, would correspond to a diffusivity $\kappa \simeq 0.2 \text{ m}^2/\text{day} \equiv 0.024 \text{ cm}^2/\text{s}$ and a correlation length $\lambda_c \simeq 4.1$ m. In comparison, $\kappa \sim 0.01 \text{ cm}^2/\text{s}$ would be the diffusivity that would be produced by microscopic swimming at speed $\sim 1 \text{ mm/s}$

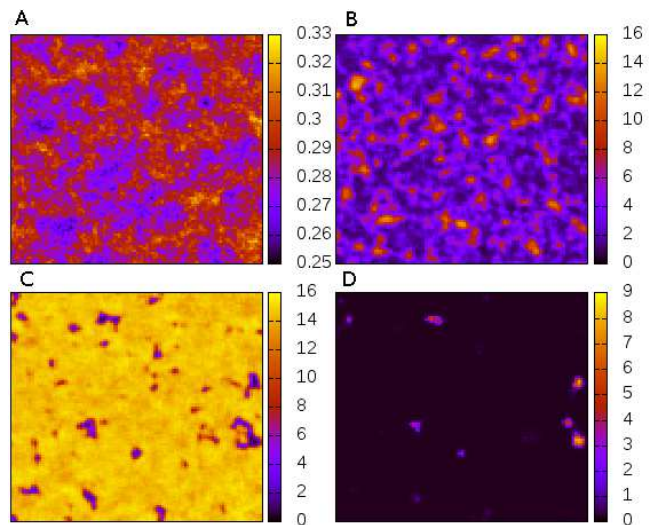


FIG. 5: Snapshots of the phytoplankton concentration field from a simulation with $\hat{m}_Z = 10^{-4}$; $\Delta T = 6^\circ\text{C}$ and other parameters set as in Eqs. (2) and (7). Size of the domain $200\Delta X \times 200\Delta X$; periodic boundary conditions, with $\Delta X = 0.3\lambda_c$. Initial conditions set equal to (P_f, Z_f) uniformly in the domain. A: day 700 (December 1st: no-bloom condition); B: day 890 (May 9th: pre-bloom condition); C: day 924 (June 13th: bloom peak); D: day 970 (July 29: concentration minimum after bloom).

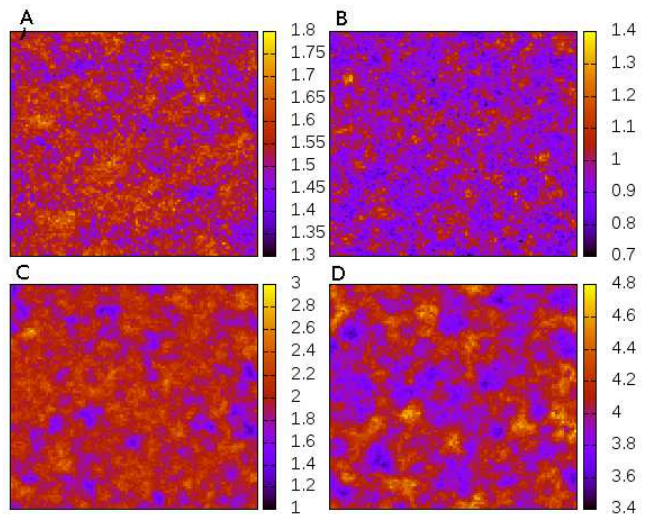


FIG. 6: Same as Fig. 5 in the case of the zooplankton field.

with a persistence time between change of directions of the order of one second [6].

As illustrated in Fig. 5, even when the system is locked globally on a bloom cycle, its dynamics is characterized by spatial fluctuations, with regions of size $\sim \lambda_c$ in which, during bloom events, P remains well below its typical bloom value.

This picture is confirmed by looking at the evolution

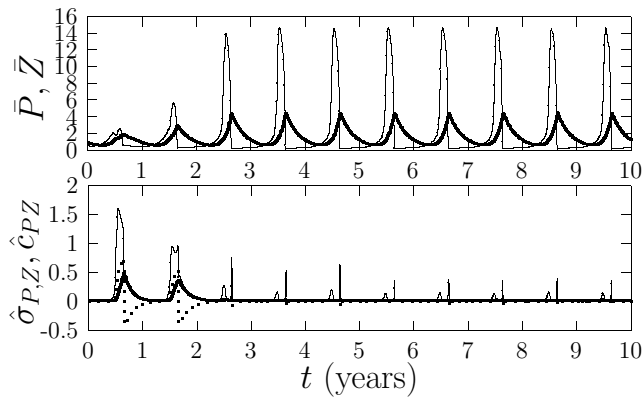


FIG. 7: Top figure: evolution of the mean concentration fields \bar{P} (thin line) and \bar{Z} (heavy line). Bottom figure: evolution of the normalized RMS fluctuations $\hat{\sigma}_P = \langle \tilde{P}^2 \rangle^{1/2} / \bar{P}$ (thin line), $\hat{\sigma}_Z = \langle \tilde{Z}^2 \rangle^{1/2} / \bar{Z}$ (heavy line), $\hat{c}_{PZ} = \text{sign}(\langle \tilde{P}\tilde{Z} \rangle) |\langle \tilde{P}\tilde{Z} \rangle| / (\bar{P}\bar{Z})^{1/2}$ (dotted line). Same choice of parameters as in Figs. 5 and 6.

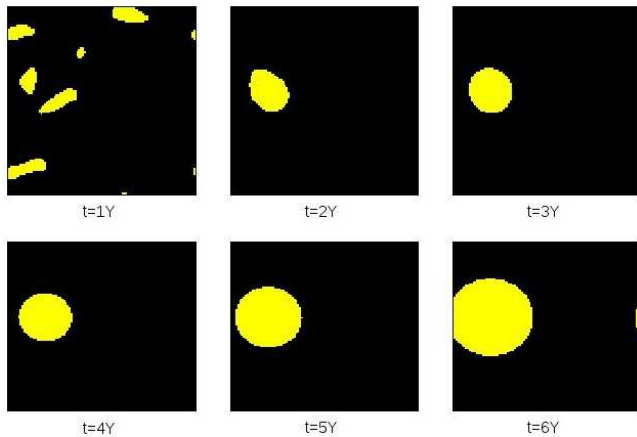


FIG. 8: Evolution due to the effect of diffusion, in the absence of noise, of domains characterized by bloom dynamics (yellow in figure; a bloom event at a given pixel is identified by crossing during the year of the threshold $P = 12$). The initial condition at $t = 0$ was a random distribution in space of values P, Z in the bloom and no-bloom basin of attraction. Initial fraction of bloom points: 0.235 (for larger fractions, the system locks immediately on a bloom-cycle; the opposite for lower fractions). Domain characteristics and parameters as in Figs. 5-6.

of the RMS fluctuations, as depicted in Fig. 7. The stronger fluctuation level in the phytoplankton concentration field, at the onset of the bloom events and soon after their disappearance, that can be seen in case *B* and *D* in Fig. 5, is paralleled by the double peaks in $\hat{\sigma}_P$ in Fig. 7.

The above picture of global destabilization of the no-bloom cycle is based on numerical evidence from simulations in a finite domain. One may question whether

destabilization could be just a finite size effect, and would disappear in the thermodynamic limit. One suggestion that this is not the case comes from the invasive character of the destabilization phenomenon. The sequence *B*–*C* in Fig. 5 gives a hint of the process: regions of size $\sim \lambda_c$, characterized by high values of P , through diffusive coupling, destabilize nearby regions with low values of P , and push them in the bloom cycle. This picture is corroborated by the behavior of the system in the noiseless $\hat{m}_Z = 0$ case. As shown in Fig. 8, in the absence of noise, the phenomenon persists: phytoplankton transfer across a $\sim \lambda_c$ distance, from a bloom to a no-bloom region, destabilizes the second one. Thus, if a bloom bubble is sufficiently large (on the scale of λ_c), it will survive diffusive transfer and gradually expand at the expenses of the surroundings. It is possible to see that the situation is confirmed in the case of a system with just two homogeneous compartments coupled diffusively, one evolving on a bloom cycle, the other on a no-bloom cycle: the no-bloom cycle will always be destabilized and the system will lock on a global bloom cycle.

This suggests the following picture:

- Demographic noise continuously generates local fluctuations in P and Z (especially in Z) that may push some regions of space in a bloom regime.
- If the noise amplitude is sufficiently high, some of these regions will be large enough for not being destroyed at once by diffusivity (see passage from year 1 to year 2 in Fig. 8).
- At this point diffusion, through phytoplankton transfer, quickly destabilizes the surrounding no-bloom regions. Noise is not expected to be important any more in this phase.

VI. CONCLUSIONS

One can imagine a hierarchy in the description of a plankton population, that goes, increasing the degree in refinement, from zero-dimensional models, to models based on the dynamics of concentration fields, such as P and Z , to individual based models (IBM), taking full account of demographic stochasticity. In some ways, PZ models (and alike) may be seen as the mean field approximation of some IBM. The correspondence between the two levels of description is established imposing that the individual reproduction probabilities in the IBM (conditional to the instantaneous local values of the concentration fields), have the same form as the corresponding mean rates at the population level.

By definition, a mean field approximation breaks-up when fluctuations are important. Usually, this means large amplitude fluctuations. If the mean-field dynamics is close to an instability, however, this is not necessarily the case, and global changes in the system can be induced by small fluctuations.

We have provided an example of such a situation in the case of a PZ model (the TB model [18]), with destabilization by demographic noise resulting in switching the system globally from a no-bloom to a bloom seasonal cycle. [The parameter determining the strength of the noise is the dimensionless constant \hat{m}_Z of Eq. (24)]. From the point of view of the PZ model, this corresponds to a decrease of the instability threshold in the seasonal temperature forcing with respect to the mean-field case (see Fig. 4). For shallow water conditions (few meters depth), and mixing in the water column produced by diffusion (diffusivity in the range $0.1 \text{ m}^2/\text{day}$), demographic noise appears sufficient to cause switching between regimes. The effect is of the same magnitude as that of the global temperature fluctuations considered in [29] (fluctuation amplitude $\sim 1^\circ\text{C}$ with correlation time equal to 35 days).

As in other systems [25, 26], the modifications of the mean-field dynamics, produced by demographic noise, are expected to be maintained in the case of an infinite system (thermodynamic limit). The reason is partly trivial: the reproduction rates at the population level are nonlinear functions of the concentration fields P and Z , and fluctuations lead necessarily to their renormalization. Such a picture, however, is incomplete, as the destabilization process, unless the demographic noise is very large, destabilizes the system only locally. [The characteristic scale of the fluctuations coincides with that of the Turing patterns of the system, and has nothing to do with stochastic demography]. Only later, by an invasive process, which appears to be insensitive to system size, the destabilized regions inglobate the inactive surroundings, leading to a global bloom cycle.

Acknowledgments

I wish to thank M. Gatto, R. Casagrandi, A. Lugliè and B. Padedda for interesting and helpful discussion. This research was funded in part by Regione Autonoma della Sardegna.

Appendix A: Master equation treatment of diffusion

We consider for simplicity a one-dimensional domain and a single species, say Z . Discretize the domain and indicate with N_i the number of individuals in slot i . We can define the PDF's:

$$\begin{aligned}\rho_{\mathbf{N}}(\mathbf{N}) &\equiv \rho_{\mathbf{N}}(\{\Omega\bar{Z}_i + \Omega^{1/2}\zeta_i, i = 1, \dots, K\}) \\ &= \Omega^{-K/2} \rho_{\zeta}(\zeta).\end{aligned}$$

Suppose that individuals are transferred diffusively from slot i to slot $i \pm 1$ with a rate $W_{i \rightarrow i+1} = W_{i \rightarrow i-1} \equiv W_i = N_i \hat{\kappa}_i$, where $\hat{\kappa}_i = \kappa_i / (\Delta x)^2$, with $\kappa_i \equiv \kappa(\mathbf{x}_i)$ the diffusivity and Δx the width of the slot. The master

equation for $\rho_{\mathbf{N}}$ can be written in the form

$$\begin{aligned}\frac{\partial \rho_{\mathbf{N}}}{\partial t} &= \sum_i \left\{ \sum_{k=\pm 1} \exp \left\{ \Omega^{-1/2} \left(\frac{\partial}{\partial \zeta_{i+k}} - \frac{\partial}{\partial \zeta_i} \right) \right\} \right. \\ &\quad \left. \times W_{i+k} - 2W_i \right\} \rho_{\mathbf{N}}.\end{aligned}\quad (\text{A1})$$

To derive an equation for $\rho \equiv \rho_{\zeta}$, we exploit the relation

$$\Omega^{K/2} \frac{\partial \rho_{\mathbf{N}}}{\partial t} = \frac{\partial \rho}{\partial t} - \Omega^{1/2} \sum_i \dot{Z}_i \frac{\partial \rho}{\partial \zeta_i}.$$

Substituting into Eq. (A1) and expanding to $O(\Omega^{-1})$, we obtain:

$$\begin{aligned}\frac{\partial \rho}{\partial t} &= \Omega^{1/2} \sum_i \dot{Z}_i \frac{\partial \rho}{\partial \zeta_i} \\ &+ \Omega \sum_i \left\{ \left[1 + \frac{1}{\Omega^{1/2}} \left(\frac{\partial}{\partial \zeta_{i-1}} - \frac{\partial}{\partial \zeta_i} \right) \right. \right. \\ &\quad \left. \left. + \frac{1}{2\Omega} \left(\frac{\partial}{\partial \zeta_{i-1}} - \frac{\partial}{\partial \zeta_i} \right)^2 \right] w_{i-1} - w_i \right\} \\ &+ \left\{ \left[1 + \frac{1}{\Omega^{1/2}} \left(\frac{\partial}{\partial \zeta_{i+1}} - \frac{\partial}{\partial \zeta_i} \right) + \frac{1}{2\Omega} \right. \right. \\ &\quad \left. \left. \times \left(\frac{\partial}{\partial \zeta_{i+1}} - \frac{\partial}{\partial \zeta_i} \right)^2 \right] w_{i+1} - w_i \right\} \rho,\end{aligned}\quad (\text{A2})$$

where we have introduced the rate density $w_i = \Omega^{-1} W_i = Z_i \hat{\kappa}_i$. Equation (A2) could be further simplified exploiting the relation

$$\sum_i [w_{i+1} + w_{i-1} - 2w_i] \rho = 0.$$

At this point we write $w_i = \bar{w}_i + \Omega^{-1/2} \hat{\kappa}_i \zeta_i$, $\bar{w}_i \equiv \hat{\kappa}_i \bar{Z}_i$, and expand Eq. (A2) in powers of Ω . We find, to $O(\Omega^{-1/2})$:

$$[\dot{Z}_i - (\bar{w}_{i+1} + \bar{w}_{i-1} - 2\bar{w}_i)] \frac{\partial \rho}{\partial \zeta_i} = 0,\quad (\text{A3})$$

which gives, taking the continuous limit $\Delta x \rightarrow 0$, the diffusion equation

$$\frac{\partial \bar{Z}(x, t)}{\partial t} = \frac{\partial^2 (\kappa(x) \bar{Z}(x, t))}{\partial x^2}.\quad (\text{A4})$$

Going to next order, we find the equation for the fluctuations

$$\frac{\partial \rho}{\partial t} = \sum_i \Pi_i \rho,\quad (\text{A5})$$

where

$$\begin{aligned}\Pi_i &= \hat{\kappa}_{i-1} \frac{\partial}{\partial \zeta_{i-1}} \zeta_{i-1} + \hat{\kappa}_{i+1} \frac{\partial}{\partial \zeta_{i+1}} \zeta_{i+1} \\ &\quad - (\hat{\kappa}_{i-1} \zeta_{i-1} + \hat{\kappa}_{i+1} \zeta_{i+1}) \frac{\partial}{\partial \zeta_i} \\ &\quad + \frac{1}{2} \left[\hat{\kappa}_{i-1} \bar{Z}_{i-1} \left(\frac{\partial}{\partial \zeta_{i-1}} - \frac{\partial}{\partial \zeta_i} \right)^2 \right. \\ &\quad \left. + \hat{\kappa}_{i+1} \bar{Z}_{i+1} \left(\frac{\partial}{\partial \zeta_{i+1}} - \frac{\partial}{\partial \zeta_i} \right)^2 \right].\end{aligned}\quad (\text{A6})$$

From Eqs. (A5-A6) we obtain the equation for the correlation $C_{ij}(t) = \langle \zeta_i(t)\zeta_j(t) \rangle$:

$$\begin{aligned} \dot{C}_{jk} = & -2(\hat{\kappa}_j + \hat{\kappa}_k)C_{jk} + \hat{\kappa}_{j-1}C_{j-1,k} + \hat{\kappa}_{k-1}C_{j,k-1} \\ & + \hat{\kappa}_{j+1}C_{j+1,k} + \hat{\kappa}_{k+1}C_{j,k+1} + \frac{1}{2}\pi_{jk} \end{aligned} \quad (\text{A7})$$

where

$$\pi_{jk} = \begin{cases} \{\bar{w}_{j-1} + 2\bar{w}_j + \bar{w}_{j+1}\}, & k = j, \\ -\{\bar{w}_{j-1} + \bar{w}_j\}, & k = j - 1, \\ 0, & k < j - 1, \end{cases}$$

and $\pi_{jk} = \pi_{kj}$. Taking the continuous limit we find that the source term π_{ij} is infinitesimal:

$$\pi_{ij} \rightarrow -4\Delta x \bar{Z}(x)\kappa(x)\delta''(x-y) \rightarrow 0,$$

and the remaining terms give the diffusion equation for $C(x, y; t) \equiv \langle \zeta(x, t)\zeta(y, t) \rangle$:

$$\begin{aligned} \frac{\partial C(x, y; t)}{\partial t} = & \frac{\partial^2(\kappa(x)C(x, y; t))}{\partial x^2} \\ & + \frac{\partial^2(\kappa(y)C(x, y; t))}{\partial y^2}. \end{aligned} \quad (\text{A8})$$

The corresponding dynamics for the fluctuation field ζ is diffusive as well:

$$\frac{\partial \zeta(x, t)}{\partial t} = \frac{\partial^2(\kappa(x)\zeta(x, t))}{\partial x^2}, \quad (\text{A9})$$

which leads to the diffusion terms to the RHS of the Langevin equations (14).

-
- [1] C.B. Field, M.J. Behrenfeld, J.T. Randerson, and P.G. Falkowski, *Science* **281**, 237 (1998)
- [2] P.J.S. Franks, *Limnol. Oceanogr.* **42**, 1297 (1997)
- [3] N. Blackburn, T. Fenchel, and J. Mitchell, *Science* **282**, 2254 (1998)
- [4] A.P. Martin, *Philos. Trans. R. Soc. London A* **365**, 2873 (2005)
- [5] R. Reigada, R.M. Hillary, M.A. Bees, J.M. Sancho and F. Sagues, *Proc. R. Soc. Lond. B* **270**, 875 (2003)
- [6] A.M. Metcalfe, T.J. Pedley and T.F. Thingstad, *J. Marine Sys.* **49**, 105 (2004)
- [7] M. Lèvy, *Lect. Notes Phys.* **774**, 219 (2008)
- [8] A. Bracco, S. Clayton and C. Pasquero, *J. Geophys. Res.* **114**, C02001 (2009)
- [9] W.J. McKiver and Z. Neufeld, *Phys. Rev. E* **83**, 016303 (2011)
- [10] P.J.S. Franks, *Limnol. Oceanogr.* **42**, 1273 (1997)
- [11] U. Siegenhalter and J.L. Sarmiento, *Nature* **356**, 589 (1993)
- [12] T.J. Smayda, *Limnol. Oceanogr.* **42**, 1137 (1997)
- [13] C.S. Yentsch, B.E. Lapointe, N. Poulton and D.A. Phinney, *Harmful Algae*, **7**, 817 (2008)
- [14] M. Scheffer, S. Rinaldi, Y.A. Kutznetsov and E.H. Van Nes, *Oikos* **80**, 519 (1997)
- [15] T.J. Smayda, *Limnol. Oceanogr.* **42**, 1132 (1997)
- [16] D.H. Cushing, *Adv. Mar. Biol.* **26**, 249 (1990)
- [17] G.T. Evans and J.S. Parslow, *Biol. Oceanogr.* **3**, 327 (1985)
- [18] J.E. Truscott and J. Brindley, *Bull. Math. Biol.* **56**, 981 (1994)
- [19] J.H. Steele and E.W. Henderson, *Am. Naturalist* **117**, 676 (1981)
- [20] M. Fasham, H. Ducklow and S. McKelvie, *J. Marine Res.* **48**, 591 (1990)
- [21] A.M. Edwards, *J. Plankton Res.* **23**, 386 (2001)
- [22] W.R. Young, A.J. Roberts and G. Stuhne, *Nature* **412**, 328 (2001).
- [23] A.J. McKane and T.J. Newman, *Phys. Rev. Lett.* **94**, 218102 (2005)
- [24] C.R. Doering, K.V. Sargsyan and L.M. Sander, *Multi-scale Modelling and Simulation* **3**, 283 (2005)
- [25] T. Butler and D. Reynolds, *Phys. Rev. E* **79**, 032901 (2009)
- [26] T. Butler and N. Goldenfeld, *Phys. Rev. E* **84**, 011112 (2011)
- [27] I. Siekmann and H. Malchow, *Math. Model. Nat. Phenom.* **3**, 114 (2008)
- [28] C.S. Holling, *Can. Entomol.* **91**, 293 (1959); C.S. Holling, *Can. Entomol.* **91**, 385 (1959)
- [29] J.A. Freund, S. Mieruch, B. Scholze, K. Wiltshire and U. Feudel, *Ecol. Complex.* **3**, 129 (2006)
- [30] J.A. Berges, D.E. Varela and P.J. Harrison, *Mar. Ecol. Prog. Ser.* **225**, 139 (2002)
- [31] E.J. González, T. Matsumura-Tundisi and J.G. Tundisi, *Braz. J. Biol.* **68**, 69 (2008)
- [32] To be precise, in order for the two species to have identical diffusion properties, we could assume that passive transport be dominant over swimming.
- [33] M. Doi, *J. Phys. A* **9**, 1465 (1976); A.S. Mikhailov, *Phys. Lett.* **85**, 214 (1981); N. Goldenfeld, *J. Phys. A* **17**, 2807 (1985); L. Peliti, *PJ. Physique* **46**, 1469 (1985); H.K. Janssen and U.C. Tauber, *Ann. Phys.* **315**, 147 (2005)
- [34] N.G. Van Kampen, *Stochastic processes in physics and chemistry* (Elsevier, New York, 1992)
- [35] S.A. Levin and L.A. Segel, *Nature* **259**, 659 (1976)